

**NASA
Technical
Paper
2520**

**AVSCOM
Technical
Report
85-B-7**

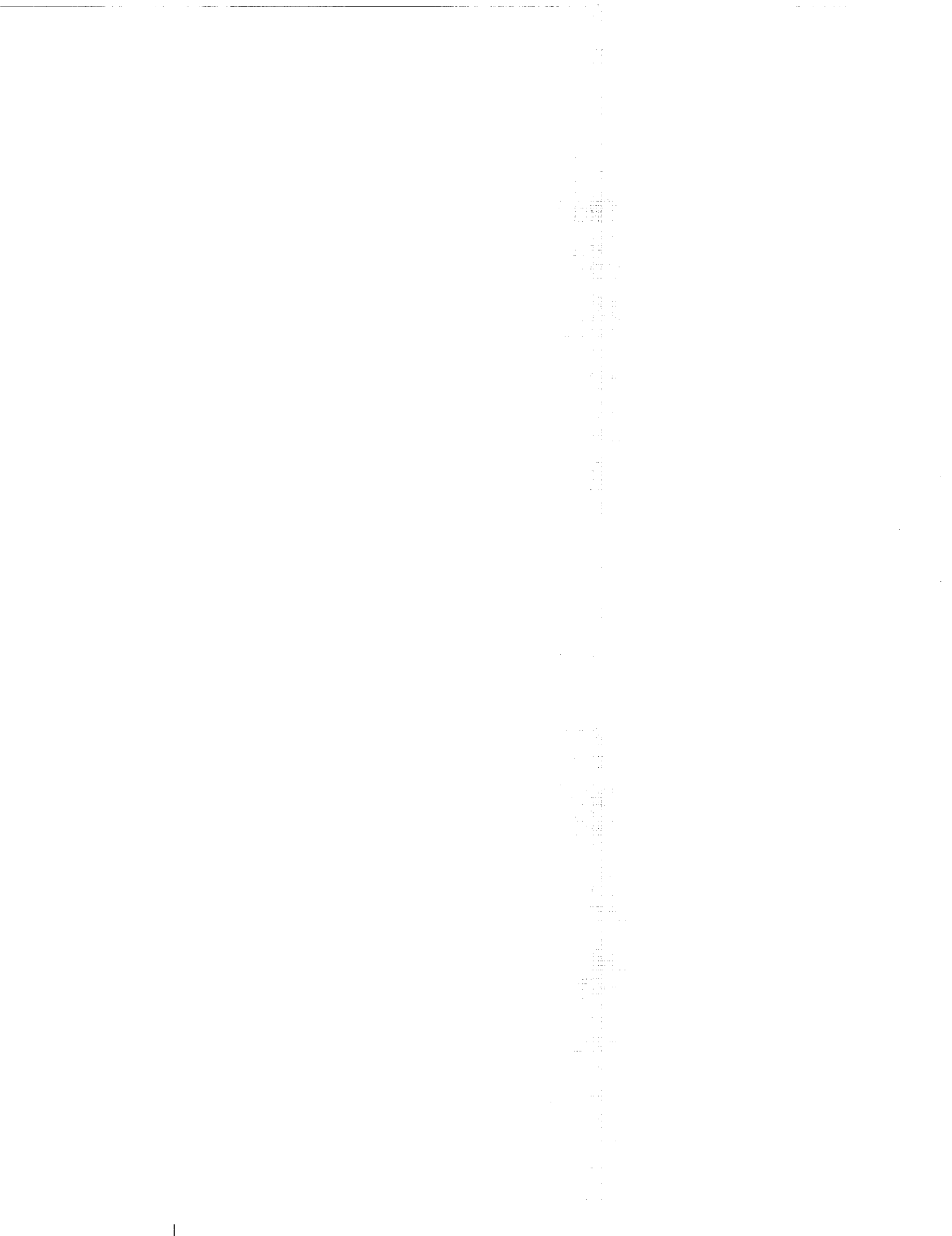
November 1985

Abrasion Behavior of Aluminum
and Composite Skin Coupons,
Stiffened Skins, and Stiffened
Panels Representative of
Transport Airplane Structures

Karen E. Jackson



NASA



**NASA
Technical
Paper
2520**

**AVSCOM
Technical
Report
85-B-7**

1985

Abrasion Behavior of Aluminum
and Composite Skin Coupons,
Stiffened Skins, and Stiffened
Panels Representative of
Transport Airplane Structures

Karen E. Jackson

*Aerostructures Directorate
USAARTA-AVSCOM
Langley Research Center
Hampton, Virginia*

NASA

National Aeronautics
and Space Administration

Scientific and Technical
Information Branch

Summary

A three-phase investigation was conducted to determine the friction and wear behavior of aluminum and composite materials under conditions similar to the loadings experienced by skin panels on the underside of a transport airplane during an emergency belly landing. In the first set of experiments, small skin coupons of aluminum and graphite-epoxy (Gr-Ep) were abraded in the laboratory. An abrasion test apparatus was designed which used a standard belt sander to provide the sliding surface. The test rig was equipped with a load cell to measure the frictional forces developed during abrasion. The skin-coupon specimens were abraded over a range of pressures (2 to 5 psi), belt velocities (16 to 50 mph), and belt surface textures (0.01 to 0.02 in.). The parameters chosen fall within the range of conditions considered typical of an airframe sliding on a runway surface. The effects of pressure and velocity on the wear rate and coefficient of dynamic friction were determined, and comparisons were made between the Gr-Ep and aluminum. Results of the laboratory tests indicate that Gr-Ep skin coupons have wear rates four to five times higher than aluminum and a coefficient of friction of about half that of aluminum.

The second phase of the investigation involved abrading more representative skin structures, consisting of I-beams with attached skins constructed of aluminum, Gr-Ep, and glass hybrid composite. These stiffened skins were abraded on an actual runway surface over the same range of pressures and velocities as in the laboratory skin-coupon tests. While the trends in the wear and friction behavior of the stiffened skins on runway surface were substantially the same as those observed in the skin-coupon tests, the magnitude of the wear rate decreased considerably for the Gr-Ep material. The coefficient-of-friction data for the two tests were in good agreement.

In the third phase of the investigation, large Gr-Ep stiffened panels which closely resembled the structure of a transport fuselage skin section were abraded on a runway surface at a pressure of 2.0 psi over a range of velocities. The data from these tests tended to correlate the stiffened-skin results.

Introduction

Friction and wear behavior of fuselage skins can be an important consideration in the design of transport aircraft, especially in the event of an emergency sliding (belly) landing on a runway surface. A review of the National Transportation Safety Board (NTSB) accident records and the Federal Aviation Administration (FAA) difficulty reports show that

21 accidents or incidents involving interference between the main landing gear tire and door have been reported since 1965, 10 of which resulted in gear-up landings (ref. 1). Reference 2 puts the number of emergency sliding landings at roughly a dozen such incidents involving transport aircraft in the last 5 years. Typically, these aircraft slide 4000 to 5000 ft with touchdown velocities of approximately 140 mph. Resulting abrasion damage to the aircraft fuselage is often quite substantial.

Composite materials are currently being used for secondary structural components and are being considered for use as primary structural components of transport aircraft. The trend in the aircraft industry towards increased application of composite materials raises the question of how these materials would behave under the conditions of a belly landing as compared with current aluminum construction.

This paper describes a three-phase investigation to study the friction and wear behavior of composite materials and aluminum under abrasive loading conditions similar to those experienced on the underside of a transport airplane during a belly landing. In the first phase (ref. 3), small skin-coupon specimens of aluminum and various advanced composite materials, including graphite-epoxy (Gr-Ep), Kevlar, and toughened-resin composites were abraded in the laboratory using a standard belt sander to provide the sliding abrasive surface to simulate a runway. The aluminum and composite skin coupons were abraded over a range of pressures (2 to 5 psi), belt velocities (16 to 50 mph), and belt surface textures (0.01 to 0.02 in.). The parameters chosen fall within the range of conditions considered typical of an airframe sliding on a runway surface. The effects of these test variables on the wear rate and coefficient of friction were determined, and comparisons were made between the aluminum and composite materials.

The second phase of the investigation (ref. 4) involved testing more representative skin structures on an actual runway. The test specimens consisted of I-beams with attached skins constructed of aluminum, graphite-epoxy, and glass hybrid composite. These stiffened skin specimens were abraded on the Langley Air Force Base north-south runway over the same range of pressures and velocities as in the laboratory skin-coupon tests. The effects of pressure and velocity on wear and friction behavior were determined for the stiffened skins and comparisons were made between the aluminum and composite materials.

In the final phase of the investigation, three large stiffened panels constructed of graphite-epoxy composite material were abraded on a runway surface at a pressure of 2.0 psi over the same range of velocities as

in previous tests. The stiffened-panel test specimen most closely resembled the construction of a transport fuselage skin section, and these tests were performed to correlate the results from the skin-coupon tests and the stiffened-skin tests.

This paper presents results from each phase of the project and shows comparisons between the friction and wear behavior of the aluminum and graphite-epoxy composite material. The paper is limited to graphite-epoxy simply because that particular composite material was tested in each phase of the investigation. More complete information on the first two phases of the project, which includes other material systems and data from temperature-time histories, may be found in references 3 and 4.

Test Apparatus and Procedures

Phase I—Skin-Coupon Tests

Specimens. A schematic of a typical skin-coupon test specimen is shown in figure 1. Thicknesses of the skin coupons varied, depending on the material, and ranged from 0.20 to 0.30 in. A 45° chamfer on the front edge of the specimen helped to smooth the initial contact of the specimen to the abrading surface. Figure 1 also lists the types of aluminum and composite materials tested, giving the lay-up of each of the composite skin-coupon specimens. Aluminum 7075-T76 is a readily available stock aluminum. The T300/5208¹ is a standard commercial graphite-epoxy composite in wide use today. Kevlar 49/934² is a popular aramid-epoxy composite, also commercially available. Three additional graphite-epoxy materials (T300/BP907, T300/Fibredux 920, and T300/Ciba 4³) chosen for testing are toughened-resin composites. As mentioned previously, although several composite-material systems other than Gr-Ep were tested, this report presents only the T300/5208 Gr-Ep and aluminum data for comparison with the stiffened-skin and stiffened-panel tests.

Apparatus. The apparatus used to perform the skin-coupon tests is shown in figures 2 and 3. A belt sander fitted with a 6-in. by 48-in. aluminum

oxide belt provided the sliding, abrasive surface. Skin-coupon test specimens were held in place by a specimen holder which was attached to the belt sander by a parallelogram arrangement of mechanical linkages. The linkages were pivoted about a back upright such that the specimen holder could be raised and lowered parallel to the abrading surface. The skin coupons fitted into a recess in the specimen holder and were held securely in place by a vacuum created behind the specimen by the vacuum pump (fig. 2).

Figure 3 shows a detailed sketch of the test apparatus in the locked (upper position) and test (lower position) configurations, where the upper position is shown by dashed lines. The specimen holder remained perpendicular to the abrading surface because of the parallelogram linkage arrangement. As the specimen wore, this arrangement kept the load normal to the abrading surface. Loads were applied to the specimen by placing lead weights on a rod attached to the specimen holder. A counterweight was used to offset any load applied to the specimen by the weight of the linkages and the specimen holder.

Instrumentation. The test apparatus was instrumented with a load cell located in the lower linkage arm (fig. 3). During abrasion testing the frictional force developed between the skin coupon and the belt produced a tensile force in the lower arm. The strain induced by this tensile force was converted by the load cell into an electrical signal which was amplified and filtered through a 10-Hz low-pass filter. The signal was then fed to a two-channel strip-chart recorder to provide a force data trace. This force measurement was used to calculate the friction and normal forces from a static analysis of the specimen holder given the applied load, the angle of inclination of the linkage arms, and the holder dimensions.

The test apparatus was also instrumented with a limit switch (fig. 2). The limit switch triggered an event marker on the strip-chart recorder when the test specimen was lowered to the abrading surface at the start of a test run. When the run was complete, the test specimen was raised, the limit switch was released, and the event marker returned to its original position. The test run time was then determined by measuring the distance between the two event marks on the strip-chart recorder and dividing that value by the chart speed.

Parameters. Typical loading conditions on the skin panels of a transport airplane during a belly landing would fall in the pressure range of 2.0 to 5.0 psi. The effect of pressure on the friction and wear behavior of the aluminum and composite skin

¹ Thornel 300 (T300) graphite fiber is manufactured by Union Carbide Corporation; 5208 epoxy resin is manufactured by Narmco Materials, a subsidiary of Celanese Corporation.

² Kevlar 49 aramid fiber is manufactured by E. I. du Pont de Nemours & Co., Inc; 934 epoxy resin is manufactured by Fiberite Corporation.

³ BP-907 epoxy resin is manufactured by American Cyanamid Corporation; Fibredux 920 and Ciba 4 epoxy resins are manufactured by Ciba Geigy Co. Ciba 4 is a specially prepared epoxy resin not available commercially.

coupons was, therefore, determined by performing separate tests at 2.0, 3.2, and 4.8 psi. These test pressures were achieved by placing 5-, 8-, and 12-lb lead weights on the rod above the specimen holder normal to the test specimen.

Standard 6-in. by 48-in. aluminum oxide belts with grit sizes ranging from No. 36 to No. 60 were used to simulate runway surfaces. This range of grit sizes was selected based on the average surface texture depths of these belts as measured with the grease sample technique (ref. 5), which has evolved as a method of classifying runway surfaces. This technique, illustrated in figure 4, involves marking a constant width on the surface to be tested and spreading a known volume of grease evenly within the marked region, filling the crevices and covering as much of the surface as possible. The volume of grease used divided by the surface area covered is the average surface texture depth.

Figure 5 (from data in ref. 5) shows the various surface types and classes of runways and the average surface-texture depths for runways within each class. The texture depth range of 0.01 to 0.02 in., shown as the shaded region in figure 5, is considered typical for runway surfaces. Therefore, to simulate a runway surface, abrasive belts with texture depths in or near this range were desired; as shown in figure 6, belts having surface textures within or near the 0.01- to 0.02-in. range were those with No. 36, No. 40, No. 50, and No. 60 grit sizes. The effect of varying the surface texture depth on the friction and wear behavior of the skin coupons was investigated in reference 3. The test results for the skin coupons presented in this paper were all performed on No. 36 grit belts.

Typical touchdown velocities of transport airplanes are approximately 140 to 160 mph. This high velocity range was unattainable with the motor drive system of the belt sander. However, by altering the pulley ratios, a range of velocities was achieved for testing. Tests at 16.0, 36.4, and 52.0 mph were performed on the aluminum and composite skin-coupon specimens at a pressure of 3.2 psi using a No. 36 grit belt.

Procedure. Prior to testing, all pertinent data such as skin-coupon initial mass and test parameters such as load, belt velocity, and belt surface-texture depth (indicated by grit size) were recorded. Skin coupons were abraded for approximately 5 seconds. This length of time was sufficient to get an adequate force data trace, yet short enough to prevent clogging of the belt with debris. Following the test, the skin-coupon mass was measured and recorded. The specimen holder and linkage assembly was then adjusted laterally to allow for another test run with a

new specimen on an unused track of the belt. In this manner, three abrasion tests were performed per belt with each test being run on a new belt surface.

Phase II—Stiffened-Skin Tests

Specimens. Figure 7 shows an aluminum specimen and a graphite-epoxy I-beam, stiffened-skin specimen with their typical dimensions, the specific skin materials, and, in the case of the Gr-Ep, the ply lay-up. The composite specimens were all fabricated with a ski front (fig. 7). The purpose of the ski was to help smooth the initial contact of the specimen with the runway surface. The aluminum stiffened skins were also outfitted with skis. Twenty stiffened-skin specimens (five each of four different material types) were fabricated. More information on this phase of the investigation is given in reference 4.

Apparatus. The apparatus used to perform abrasion tests on the I-beam stiffened skins is shown in figures 8 and 9. The integrated tire test vehicle (ITTV) was used to tow the runway abrasion test trailer with the test apparatus mounted on it (fig. 8). Figure 9 is a detailed view of the runway abrasion test trailer and apparatus. The design and operation of the apparatus to conduct the stiffened-skin tests is similar in concept to that used for the test apparatus for the skin-coupon tests. The specimens were held in place by securing the top flange to a holder which was attached to a parallelogram arrangement of mechanical linkages consisting of a large top beam, a rigid central support, a lower linkage arm, and the specimen holder. These four members were connected by pinned joints so that the specimen holder could be raised and lowered to the runway surface by pivoting the top beam. The specimen holder remained perpendicular to the runway surface because of the parallelogram linkage arrangement. As the skin of the I-beam specimen wore, this arrangement ensured that the load remained normal to the abrading surface. Loads were applied to the stiffened-skin specimen by placing lead weights on the specimen holder (fig. 9).

A hydraulic system (fig. 9) was mounted to the trailer to control the action of the mechanical linkages in lowering and raising the test specimens to the runway surface. The system consisted of a pump, an accumulator, a four-way valve, and a hydraulic cylinder. To lower the stiffened skin, the hydraulic system was actuated such that the hydraulic cylinder extended, thereby releasing the cable attached through a pulley to the top beam of the linkage assembly. The system worked in reverse to raise the test specimen.

Operation of the abrasion tests was automated through a control circuit which, when initiated by an operator in the ITTV cab, programmed the hydraulic system to lower the stiffened-skin specimen to the runway surface and start the data recording devices at specific intervals. The test specimens were abraded for approximately 6 seconds, at which time the hydraulic system automatically raised them from the runway surface and shut off the data recorders. The control circuit and all data recording devices operated off the onboard power generator of the ITTV.

Instrumentation. The test apparatus was instrumented with a load cell located in the lower linkage arm (fig. 9). During abrasion testing the frictional force developed between the stiffened skin and the runway produced a tensile force in the lower arm. The signal generated from the load cell was amplified and filtered through a 2-Hz low-pass filter. The signal was then fed to a two-channel strip-chart recorder to provide a force data trace. This force measurement was used to calculate the coefficient of dynamic friction in the same manner as in the skin-coupon tests. The test apparatus was also instrumented with a limit switch (fig. 9). The limit switch triggered an event marker on the strip-chart recorder to signify when the stiffened skin was in contact with the ground. The run time of the test was determined by measuring the length between the two event marks on the strip-chart recorder and dividing that value by the known chart speed. The strip-chart recorder, filter, amplifier, and other data recording devices were mounted to the test trailer as shown in figure 9.

Parameters. The effect of pressure on specimen wear behavior and coefficient of friction was determined for the aluminum and Gr-Ep stiffened skins at pressures of 2.0, 3.2, and 5.0 psi. These tests were conducted at a test velocity of 32.5 mph such that pressure was the only variable in the series of tests, except for the natural variations in the runway surface. These conditions are similar to those used in the skin-coupon tests to determine the effect of pressure on friction and wear behavior.

Unlike the skin coupon tests, which were performed in the laboratory using a belt sander to simulate a runway surface, the stiffened-skin tests were conducted on an actual runway surface. The tests were performed on the Langley Air Force Base north-south runway located in Hampton, Virginia. This runway is a concrete surface and has a measured surface texture depth of 0.011 in., which is typical of heavily textured concretes and the majority of harsher types of asphalt (ref. 5).

The high velocity range (140 to 160 mph) required to accurately simulate the touchdown velocities of a transport airplane was unattainable with the ITTV-towed abrasion trailer and test apparatus. However, a range of velocities was chosen for testing purposes. Tests at 16.0, 32.5, and 45.0 mph were performed on the aluminum and Gr-Ep stiffened-skin specimens at a pressure of 3.2 psi. These conditions are similar to those used in the skin-coupon tests to determine the effect of velocity on friction and wear behavior.

Procedure. All pertinent data, such as test-specimen dimensions and mass, and test parameters, such as load and velocity, were recorded prior to testing. The weight necessary to achieve the desired test pressure was attached to the specimen holder. The test operator activated the control circuit to begin the test from a remote switch inside the ITTV cab, once the test velocity had been achieved. The driver of the ITTV maintained this speed for approximately 15 seconds to ensure constant velocity during the entire run time of the test. Following the test, the stiffened-skin mass was recorded, and the force data trace was removed and labeled. This procedure was repeated for each test.

Phase III—Stiffened-Panel Tests

Specimens. The third phase of the investigation involved abrading three stiffened panels constructed of Gr-Ep composite material. A typical panel is shown in figure 10. The panel consisted of a 24-in. by 24-in. skin constructed of AS4/3502⁴ Gr-Ep composite material with a lay-up (fig. 10). The panel was stiffened in the sliding direction by three, 1-in. high Z-stringers and was stiffened in the perpendicular direction by two, 5-in. high Z-frames. These tests were performed to correlate the results from the two previous phases and to provide the most realistic simulation of the transport skin structure for wear and friction testing.

Apparatus and procedure. The apparatus used to perform the stiffened-skin tests in phase II of the investigation was modified to accommodate the larger panel test specimens. The specimen holder was altered so that the stiffened panels were held to it by the top flanges of the Z-frames. Also, a higher capacity load cell was installed in the lower linkage arm in anticipation of the higher loads caused by the larger panel size. The same data recording system and hydraulic control system were used to conduct

⁴ AS4/3502 graphite-epoxy composite is a prepreg manufactured by Hercules Incorporated.

the tests. The test procedure was the same as used in the stiffened-panel tests.

The stiffened-panel tests were performed at a pressure of 2.0 psi and at velocities of 16.0, 32.5, and 45.0 mph. Except for the fact that a lower pressure level was used for these tests, these conditions are similar to those used to determine the effect of velocity on wear and friction behavior of the skin coupons and stiffened skins. The large loads introduced into the test apparatus by applying the amount of weight required to obtain the 3.2-psi pressure level used in the skin-coupon and stiffened-skin tests were prohibitive for the stiffened-panel tests.

Results and Discussion

Abrasion Surface Description

Skin coupons. The general appearance of the abraded wear surface and the wear debris of the skin coupons are shown in figure 11. The wear surface of the aluminum specimen contained thin, evenly spaced grooves along the direction of sliding. Aluminum wear debris consisted of small particles having a powder-like texture. The graphite-epoxy specimen exhibited a wear surface similar to the aluminum specimen, although the Gr-Ep surface was smoother and the grooves were not quite as deep. Wear debris from these specimens consisted mainly of fine particles interspersed with some pieces of broken fibers. The abraded surface of a Kevlar specimen is also depicted, though the Kevlar skin-coupon results are not presented in this paper.

Stiffened skins. Figure 12 shows the general appearance of the abraded surface for a typical aluminum specimen, a graphite-epoxy specimen, and two glass hybrid composite stiffened-skin specimens. The wear surface of the aluminum specimen contained rough, jagged grooves which were fairly regularly spaced along the direction of sliding. The grooves were more widely separated and more shallow than those observed in the aluminum skin coupons. The Gr-Ep stiffened skins exhibited a wear surface with similar long groove marks. These grooves were smoother than for the aluminum specimen, but were more irregularly spaced and less deep than those of the Gr-Ep skin coupons. In both the skin-coupon and stiffened-skin tests, the wear appeared to be fairly uniform over the skin area.

Stiffened panel. The wear surface for one of the stiffened panels is shown in figure 13. The surface contained irregularly spaced long and short gouges which were wider than those in either the Gr-Ep skin

coupons or stiffened skins. The wear was heaviest towards the front of the specimen, nearest the ski. Also, the runway appeared to be undamaged from the stiffened-skin and stiffened-panel abrasion tests.

Wear Behavior

In the following sections, the effects of independently varying the pressure and velocity on the wear behavior of the skin coupons, stiffened skins, and stiffened panels are discussed, and comparisons are made between the aluminum and Gr-Ep composite material. In particular, the discussions are centered on how the specimen wear rate and wear index are affected by the test variables. The wear rate is defined as the average reduction in specimen thickness per unit of run time and is calculated from the following equation:

$$\text{Wear rate} = \frac{m_i - m_f}{\rho l w (t_r)}$$

where

m_i initial mass

m_f final mass

ρ density of skin material

l specimen length

w specimen width

t_r run time

Thus, wear rate is computed in dimensions of inches per second. A means of nondimensionalizing the results is to divide the wear rate by the test velocity. This parameter is called the wear index and is computed from the following equation:

$$\text{Wear index} = \frac{\text{Wear rate}}{\text{Velocity}}$$

Effect of pressure. The wear rate as a function of normal pressure is shown in figures 14 and 15 for the aluminum and Gr-Ep skin specimens, respectively. A least-squares linear curve fit was made through the data points, since a linear relationship appeared to best represent the trends in the data. The data for the skin coupons, stiffened skins, and stiffened panels are given in tables I, II, and III, respectively. Each data point in table I represents the average of 2 to 3 separate tests, whereas the data in tables II and III for the stiffened skins and stiffened panels represent a single test.

The wear rate increased as a linear function of load for both the aluminum and the Gr-Ep specimens. In the case of the aluminum (fig. 14), the

stiffened skins showed a 20- to 40-percent decrease in wear rate at each pressure level. However, the Gr-Ep stiffened skins exhibited a much greater decrease, approximately 75 percent, at each pressure level. This dramatic difference is depicted in the bar chart of figure 16. At each pressure level, the Gr-Ep skin-coupon wear rate is several times greater than the wear rates for the other test specimens.

The large decrease in wear rate between the Gr-Ep skin coupons, stiffened skins, and stiffened panels is probably the result of a combination of two factors. First, the skin-coupon specimens were abraded on aluminum oxide abrasive belts having a surface texture similar to a typical runway. However, the surface texture depth measurement does not indicate in any way that the roughness characteristics of the two surfaces are similar. In fact, they are very different. The aluminum oxide belt was a uniform, sharp, jagged surface which wore the specimens in very fine, regularly spaced grooves. The runway was a highly nonuniform surface with irregularly spaced rocks and small gravel imbedded in the concrete surface. This resulted in the more shallow and irregularly spaced groove patterns on the stiffened-skin specimens. The difference in roughness and surface quality between the belt surface and the actual runway may account, in part, for the decrease in wear rate between the Gr-Ep skin coupons and stiffened skins. This factor may also account for the difference in the behavior of the aluminum specimen; however, the aluminum appears to be much less sensitive to the difference in surface quality than the Gr-Ep.

The second factor which may have influenced the wear behavior is a combination of specimen size and the resulting problems of uniform wear and loading. Skin area increased by an order of magnitude from the skin-coupon specimens to the stiffened skins and again from the stiffened skins to the stiffened panels. Increasing the specimen size made obtaining even pressure and uniform wear more difficult. Adjustments were made to test apparatus for the skin-coupon specimens to insure uniform wear and loading. Adjustments were also made to the test apparatus used for the stiffened-skin and stiffened-panel tests. However, for the stiffened-panel tests, the specimen would not sit flat because of the curvature of the runway. This condition may have contributed to the decrease in wear rate with specimen size. Since an aluminum stiffened panel was not tested, the size effect cannot be fully determined. In observing the wear patterns of the Gr-Ep specimens, it is obvious that the stiffened panels did not have uniform contact with the runway surface.

Effect of velocity. The effect of velocity on wear rate is shown in figures 17 and 18 for the aluminum and Gr-Ep skin specimens, respectively. A linear least-squares curve-fit technique was used to plot trends in the data. The wear rate increased with velocity for both the aluminum and Gr-Ep skin specimens; however, for both materials, the skin coupons exhibited the greatest rate of increase of wear rate with velocity. As the skin area increased, the wear rate became less sensitive to changes in test velocity. In fact, the wear rate of the Gr-Ep stiffened panels remained almost constant throughout the velocity range. In general, the aluminum specimens had wear rates 2 to 5 times less than their Gr-Ep counterparts. This difference is shown graphically in the bar chart of figure 19. The Gr-Ep skin-coupon wear rate was several times that of the other test specimens. This same trend is seen in the plot of wear rate versus pressure (fig. 16).

Figures 20 and 21 are plots of the wear index versus velocity for the aluminum and Gr-Ep test specimens, respectively. For the skin coupons, both aluminum and Gr-Ep, the wear index increased with velocity. The stiffened skins and stiffened panels exhibited the opposite behavior and tended to decrease with velocity. The differences between the wear index at each velocity of the various test specimens are depicted in a bar chart in figure 22. The Gr-Ep skin-coupon wear index is several times greater than that of the other test specimens because of its higher wear rate at each velocity.

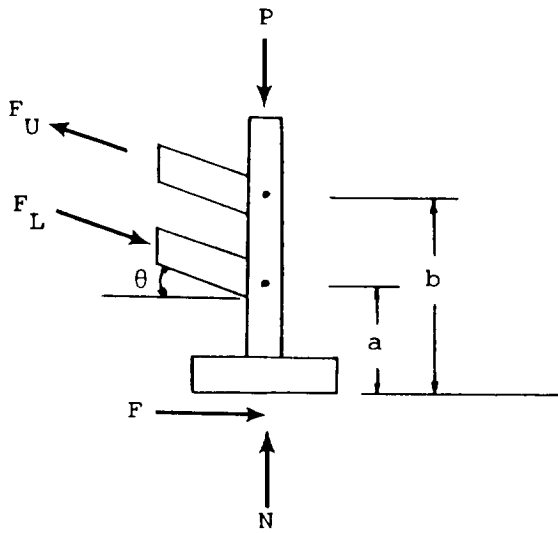
Coefficient-of-Friction Data

The frictional forces developed between the test specimen and the sliding abrasive surface (belt or runway) were calculated from a static analysis of the specimen holder (sketch A) given the applied load P , the angle of inclination of the linkage arms θ , and the force output measured from the load cell F_L . The coefficient of friction μ is derived from the computed frictional force based on the measured force in the lower linkage arm. Summation of the moments yields

$$F = F_L(\cos \theta) \left(\frac{a}{b} - 1 \right)$$

Summation of the forces in the horizontal and vertical directions yields

$$N = P + F_L(\sin \theta) \left(1 - \frac{a}{b} \right)$$



Sketch A

Therefore, the coefficient of friction is given by

$$\mu = \frac{F}{N} = \frac{F_L(\cos \theta) \left(\frac{a}{b} - 1 \right)}{P + F_L(\sin \theta) \left(1 - \frac{a}{b} \right)}$$

In the following sections, the effect of pressure and velocity on the coefficient of friction is presented. The data for the skin coupons, stiffened skins, and stiffened panels are given in tables I, II, and III, respectively.

Effect of pressure. The effect of normal pressure on the coefficient of friction for the aluminum and Gr-Ep test specimens are plotted in figures 23 and 24, respectively. A least-squares linear curve fit was made through the points. The data indicate that there are no clear trends in the behavior of the coefficient of friction as a function of pressure. For the stiffened-skin tests, the coefficient of friction increased with pressure for both the aluminum and Gr-Ep materials. However, it tended to decrease slightly for the skin-coupon tests. Figure 25 shows the coefficient-of-friction data presented as a bar chart. This figure indicates, perhaps better than the graphs, that the aluminum specimens tended to have coefficients of friction of about 0.20 and that the Gr-Ep specimens tended to have coefficients of friction in the range of 0.10 to 0.15, or approximately half that of aluminum. These data suggest that during an airplane belly landing, a transport with a Gr-Ep composite skin may slide twice as far as a similar transport with an aluminum skin.

Effect of velocity. Figures 26 and 27 show the variation in coefficient of friction with velocity for

the aluminum and Gr-Ep test specimens. As with the plots of coefficient of friction versus pressure, no consistent trends in the data are apparent. Again, the data indicate that the aluminum coefficient of friction is approximately 0.20 and that the Gr-Ep coefficient of friction ranges from 0.10 to 0.15. This point is emphasized graphically in figure 28.

Concluding Remarks

The objective of this investigation was to compare the friction and wear response of aluminum and graphite-epoxy (Gr-Ep) composite materials when subjected to loading conditions similar to those experienced by the skin panels on the underside of a transport airplane during an emergency sliding landing on a runway surface. A three-phase experimental program was conducted to simulate these conditions. The first phase involved a laboratory test which used a standard belt sander to provide the sliding abrasive surface. Small skin-coupon test specimens were abraded over a range of pressures and velocities to determine the effects of these variables on the coefficient of friction and wear rate. The second phase involved abrading I-beam stiffened skins on an actual runway surface over the same range of pressures and velocities used in the first phase. In the third phase, large stiffened panels, which most closely resembled transport fuselage skin construction, were abraded on a runway surface.

Comparisons were made between the aluminum and the Gr-Ep composite materials and between the laboratory controlled tests and those conducted on a runway surface. Major findings of this investigation include:

1. Wear rate for both the aluminum and graphite-epoxy materials was a linearly increasing function of load and velocity.
2. For each specimen type, skin-coupon and stiffened-skin, the Gr-Ep specimens had wear rates two to five times higher than their aluminum counterparts.
3. The coefficient of friction for the Gr-Ep specimens was approximately half that of aluminum.
4. Wear behavior of the skin-coupon tests performed in the laboratory on abrasive belts to simulate a runway surface did not correlate well with the wear behavior of the stiffened-skin or stiffened-panel tests performed on an actual runway surface. Wear under laboratory test conditions was several times greater than that experienced on the runway.

NASA Langley Research Center
Hampton, VA 23665-5225
September 9, 1985

References

1. NTSB Incident File, Miami, Florida. Boeing B-727-200, N8831E, Feb. 15, 1983, MIA-83-I-A075.
2. Passengers Praise Pilot for Actions in Accident. *Times-Herald* (Newport News, Va.), 83rd year, no. 71, Mar. 24, 1983. p. 13.
3. Jackson, Karen E.: *Friction and Wear Behavior of Aluminum and Composite Airplane Skins*. NASA TP-2262. AVSCOM TR 83-B-7, 1984.
4. Jackson, Karen E.: *Friction and Wear Behavior of Aluminum and Composite I-Beam Stiffened Airplane Skins*. NASA TM-86418, USAAVSCOM TM 85-B-2, 1985.
5. Yager, Thomas J.; Phillips, W. Pelham; Horne, Walter B.; and Sparks, Howard C. (appendix D by R. W. Sugg): *A Comparison of Aircraft and Ground Vehicle Stopping Performance on Dry, Wet, Flooded, Slush-, Snow-, and Ice-Covered Runways*. NASA TN D-6098, 1970.

TABLE I. TEST RESULTS OF PHASE I: SKIN-COUPON TESTS

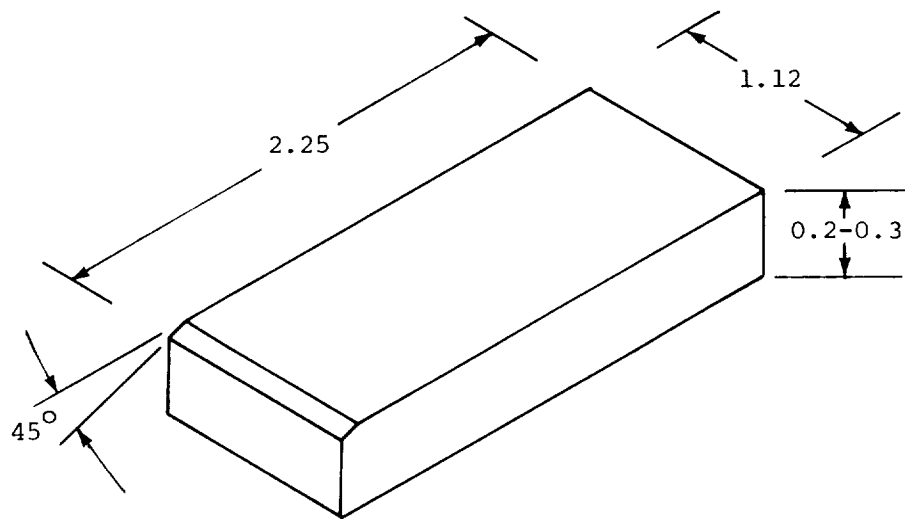
Test	Material	Test pressure, psi	Test velocity, mph	Wear rate, in./sec $\times 10^{-3}$	Wear index, in./in. $\times 10^{-6}$	Coefficient of friction
1	Aluminum ↓	2.0	36.4	0.80×10^{-3}	1.25×10^{-6}	0.21
2		3.2	16.0	.80	2.84	.19
3		3.2	36.4	1.20	1.87	.19
4		3.2	52.0	2.80	3.06	.19
5		4.8	36.4	2.40	3.75	.20
6	Gr-Ep ↓	2.0	36.4	4.00	6.24	.14
7		3.2	16.0	2.80	9.94	.12
8		3.2	36.4	7.60	11.9	.12
9		3.2	52.0	12.0	13.1	.12
10		4.8	36.4	13.6	21.2	.12

TABLE II. TEST RESULTS OF PHASE II: STIFFENED-SKIN TESTS

Test	Material	Test pressure, psi	Test velocity, mph	Wear rate, in./sec	Wear index, in./in.	Coefficient of friction
1	Aluminum ↓	2.0	32.5	0.50×10^{-3}	0.86×10^{-6}	No data
2		3.2	16.0	.57	2.03	0.18
3		3.2	32.5	.92	1.60	.19
4		3.2	45.0	.93	1.18	.23
5		5.0	32.5	1.76	3.07	.24
6	Gr-Ep ↓	2.0	32.5	1.08	1.88	.06
7		3.2	16.0	1.57	5.55	.15
8		3.2	32.5	1.79	3.13	.10
9		3.2	45.0	2.95	3.72	.14
10		5.0	32.5	3.76	6.55	.15
11	Hybrid 1 ↓	2.0	32.5	1.28	2.23	.10
12		3.2	16.0	2.73	9.69	.10
13		3.2	32.5	1.91	3.33	.10
14		3.2	45.0	2.12	2.67	.11
15		5.0	32.5	3.85	6.71	.19
16	Hybrid 2 ↓	2.0	32.5	1.57	2.73	.08
17		3.2	16.0	1.08	3.84	.09
18		3.2	32.5	.91	1.59	.13
19		3.2	45.0	2.51	3.16	.08
20		4.1	32.5	2.36	4.12	.17

TABLE III. TEST RESULTS OF PHASE III: STIFFENED-PANEL TESTS

Test	Material	Test pressure, psi	Test velocity, mph	Wear rate, in./sec	Wear index, in./in.	Coefficient of friction
1	Gr-Ep	2.0	16.0	0.23×10^{-3}	0.81×10^{-6}	0.10
2	Gr-Ep	2.0	32.5	.36	.62	.09
3	Gr-Ep	2.0	45.0	.43	.54	.12



TEST MATERIALS

Material	Lay-up
Aluminum: 2024-T4	
Composite: T300/5208 Kevlar 49/934	$(\underline{+45/0/90}/\bar{+45/0/90})_{3S}$ $(\underline{+45/0}_2/\underline{+45/0}_2/\underline{+45/0/90})_{2S}$
T300/BP-907	
T300/Fibredux 920	
T300/Ciba 4	

Figure 1. Schematic of a typical skin-coupon abrasion test specimen and a list of types of aluminum and composite materials used in abrasion tests. Drawing dimensions are in inches unless otherwise noted.



L-83-1393

Figure 2. Abrasion test apparatus for skin-coupon tests.

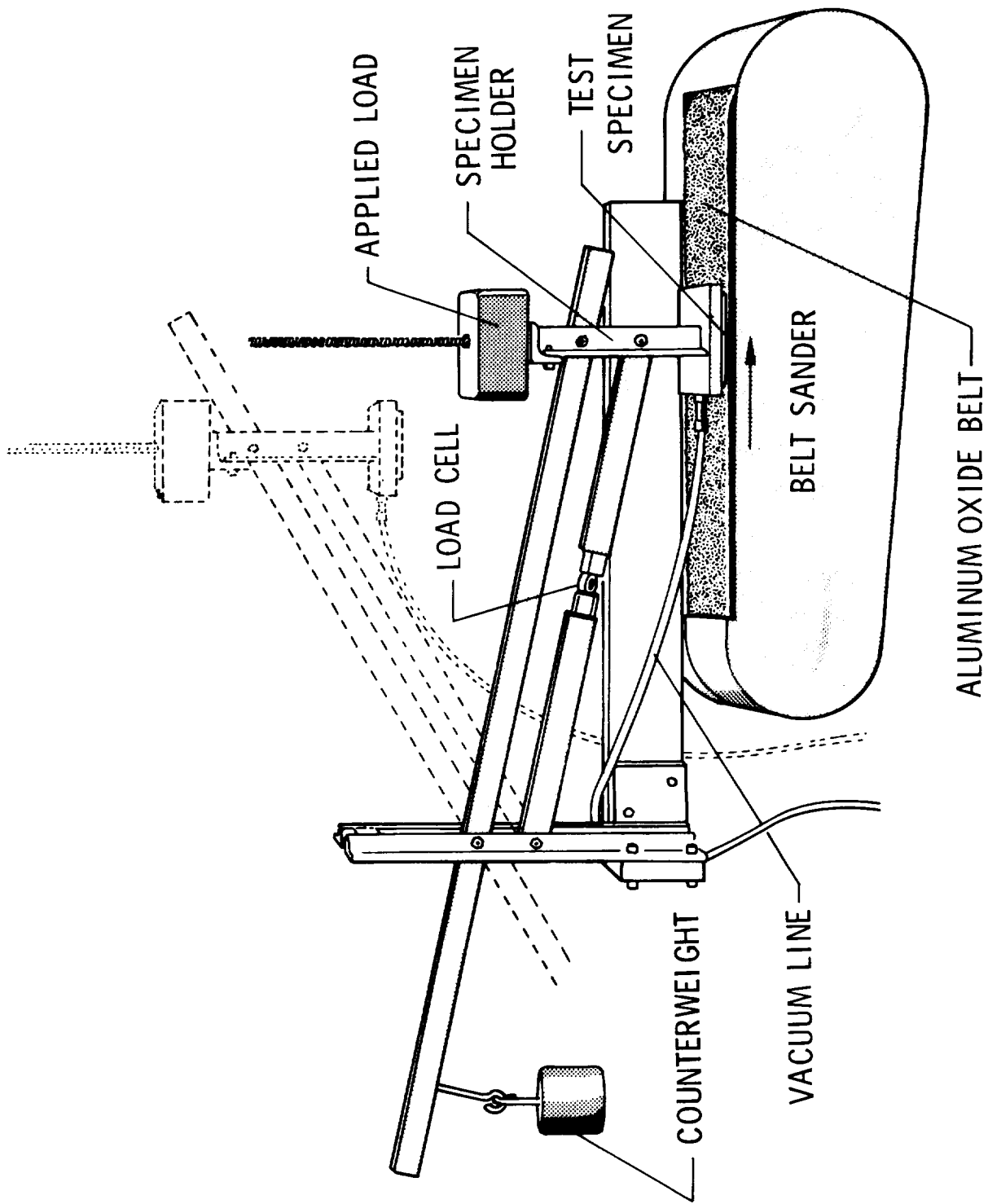


Figure 3. Schematic of skin-coupon test apparatus depicting parallelogram arrangement of linkage arms.



L-83-2538

Figure 4. Illustration of grease sample technique to determine texture depth of aluminum oxide grit belts.

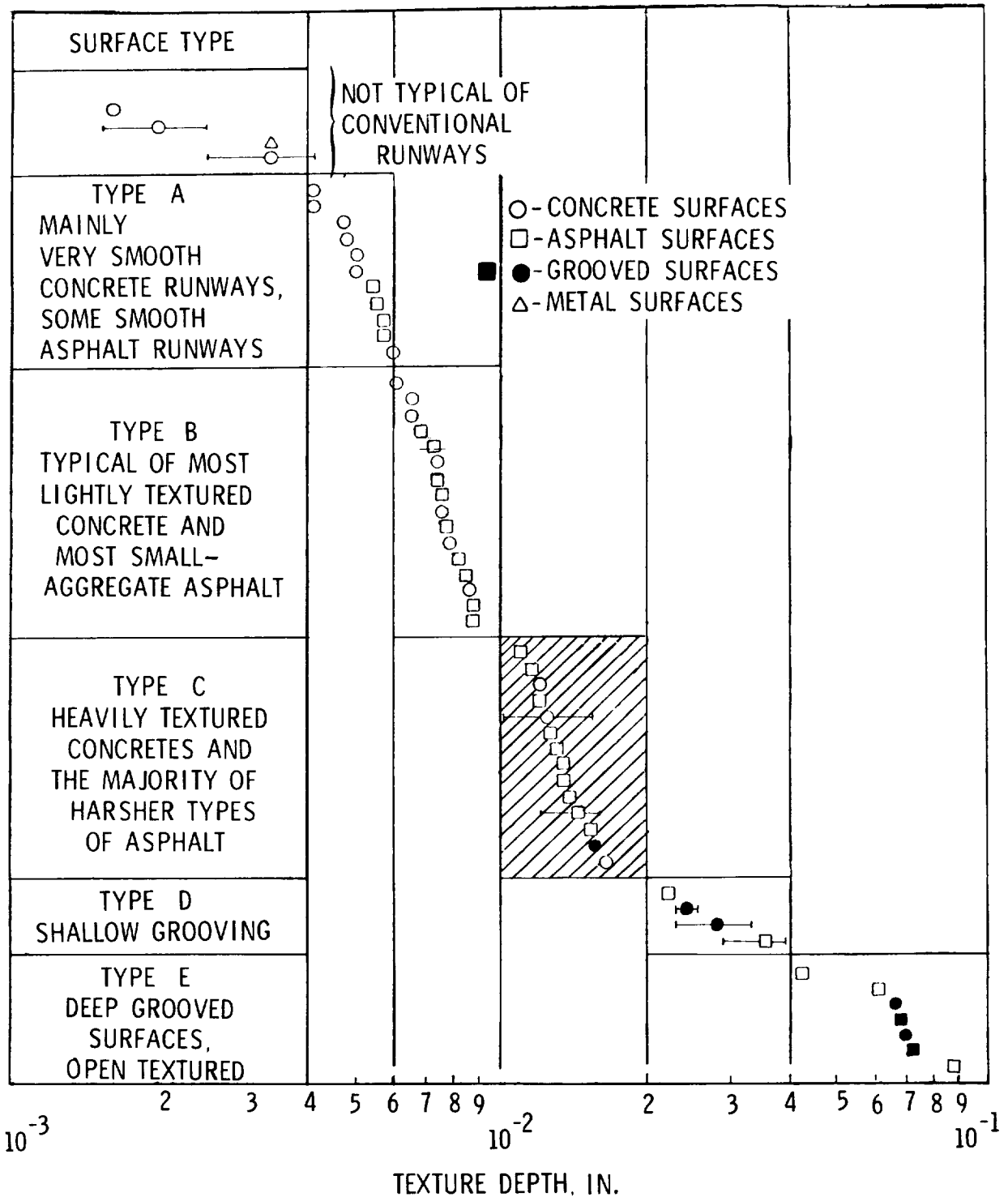


Figure 5. Classification of runway surfaces. Texture depths measured by grease or sand patch methods. (From data in ref. 5.)

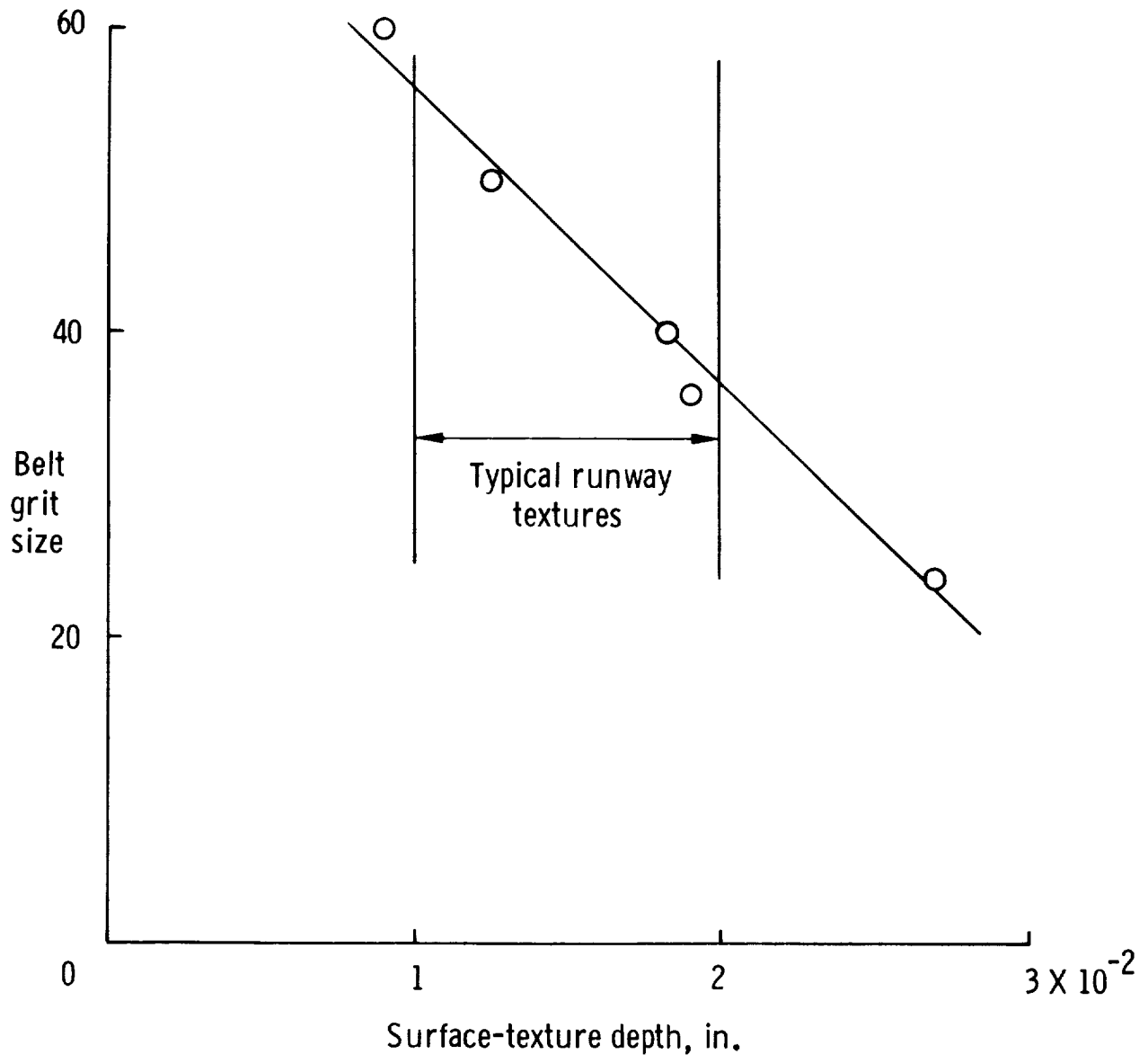
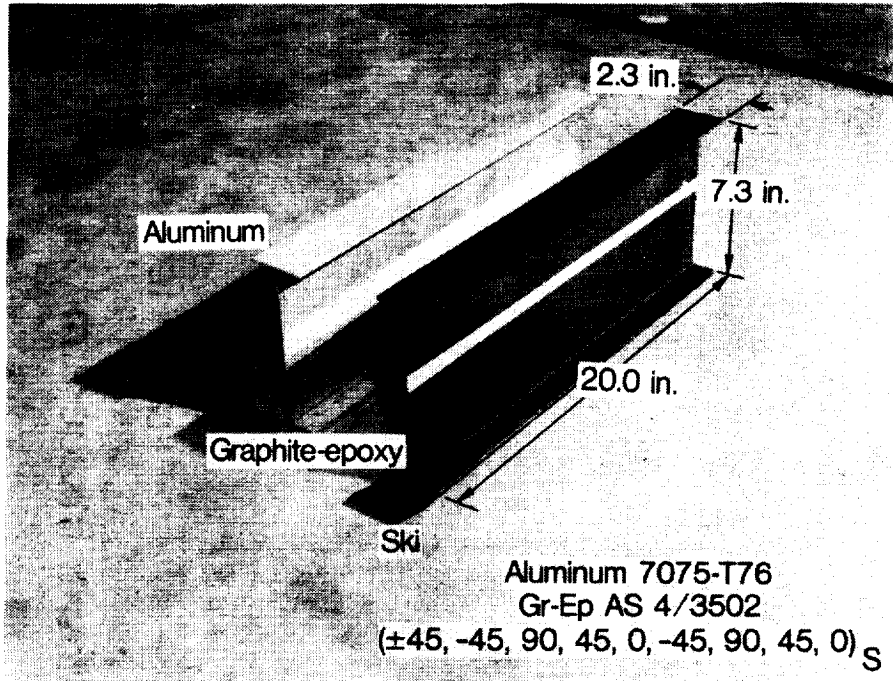
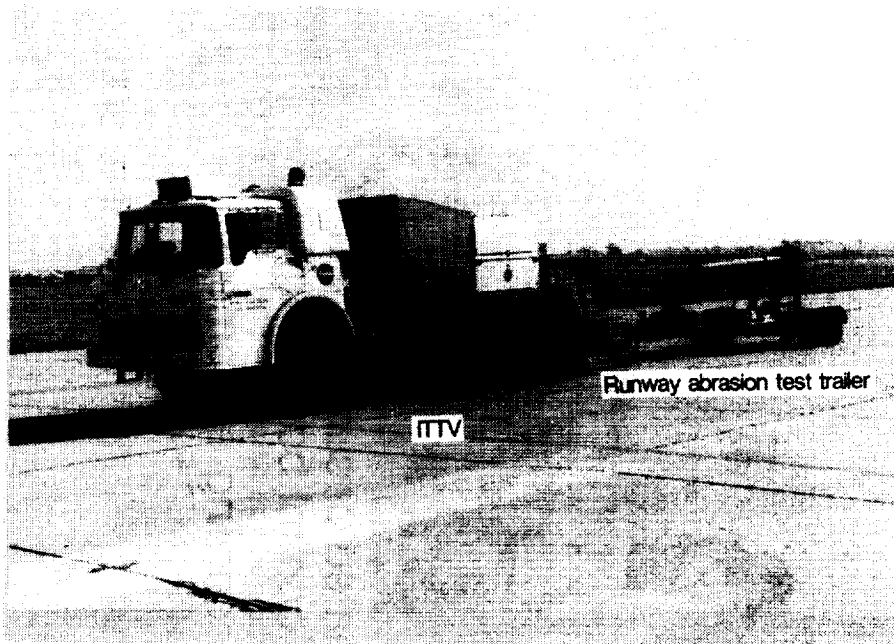


Figure 6. Results of performing grease sample technique on aluminum oxide belts. Belts lying in the typical range were used in abrasion testing.



L-85-150

Figure 7. I-beam stiffened-skin test specimen.



L-85-151

Figure 8. Abrasion test trailer towed by integrated tire test vehicle (ITTV) on Langley north-south runway.

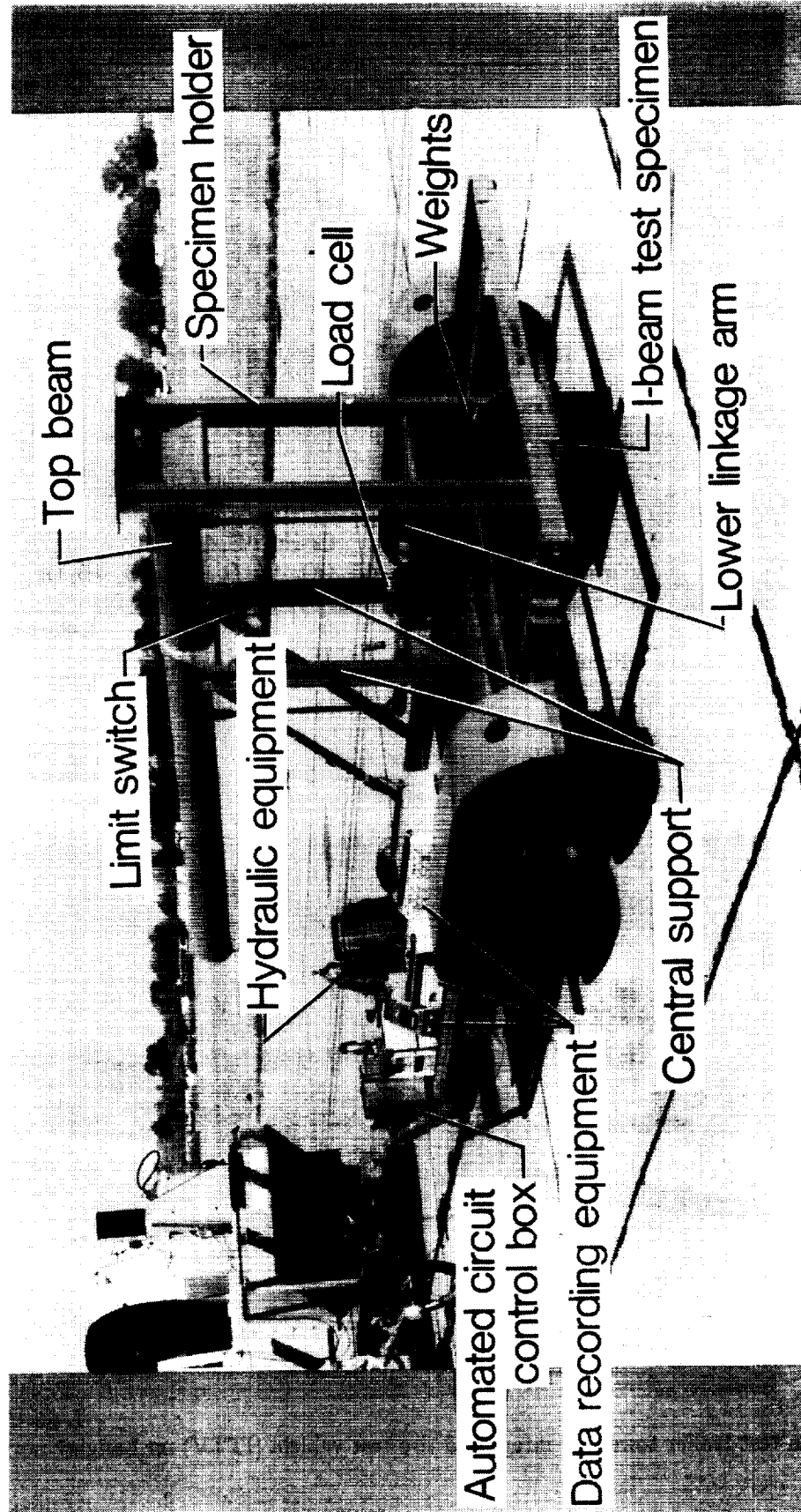
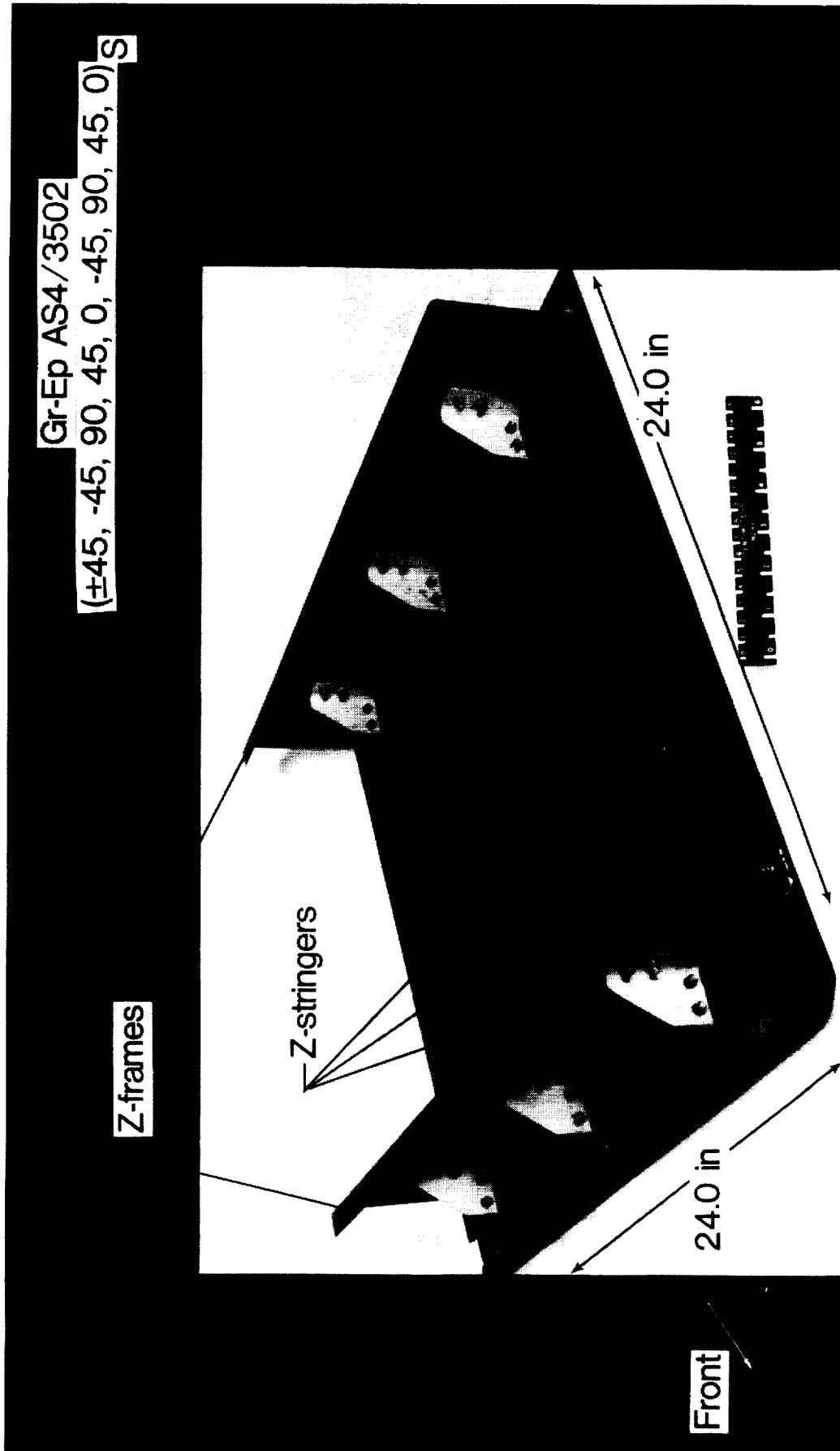


Figure 9. Abrasion test trailer and apparatus for stiffened-skin and stiffened-panel tests.

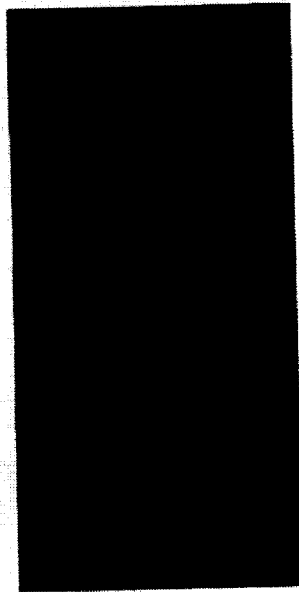


L-84-13,733

Figure 10. Graphite-epoxy stiffened-panel test specimen.



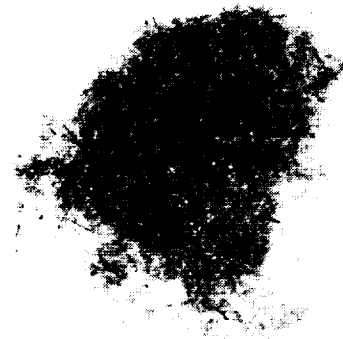
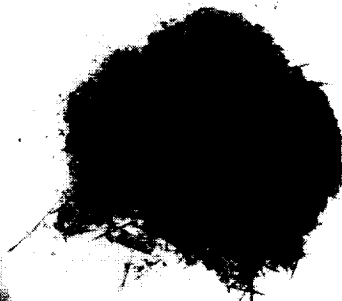
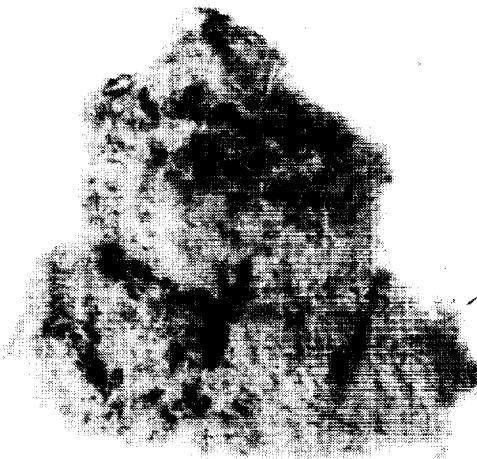
Kevlar



Graphite-Epoxy

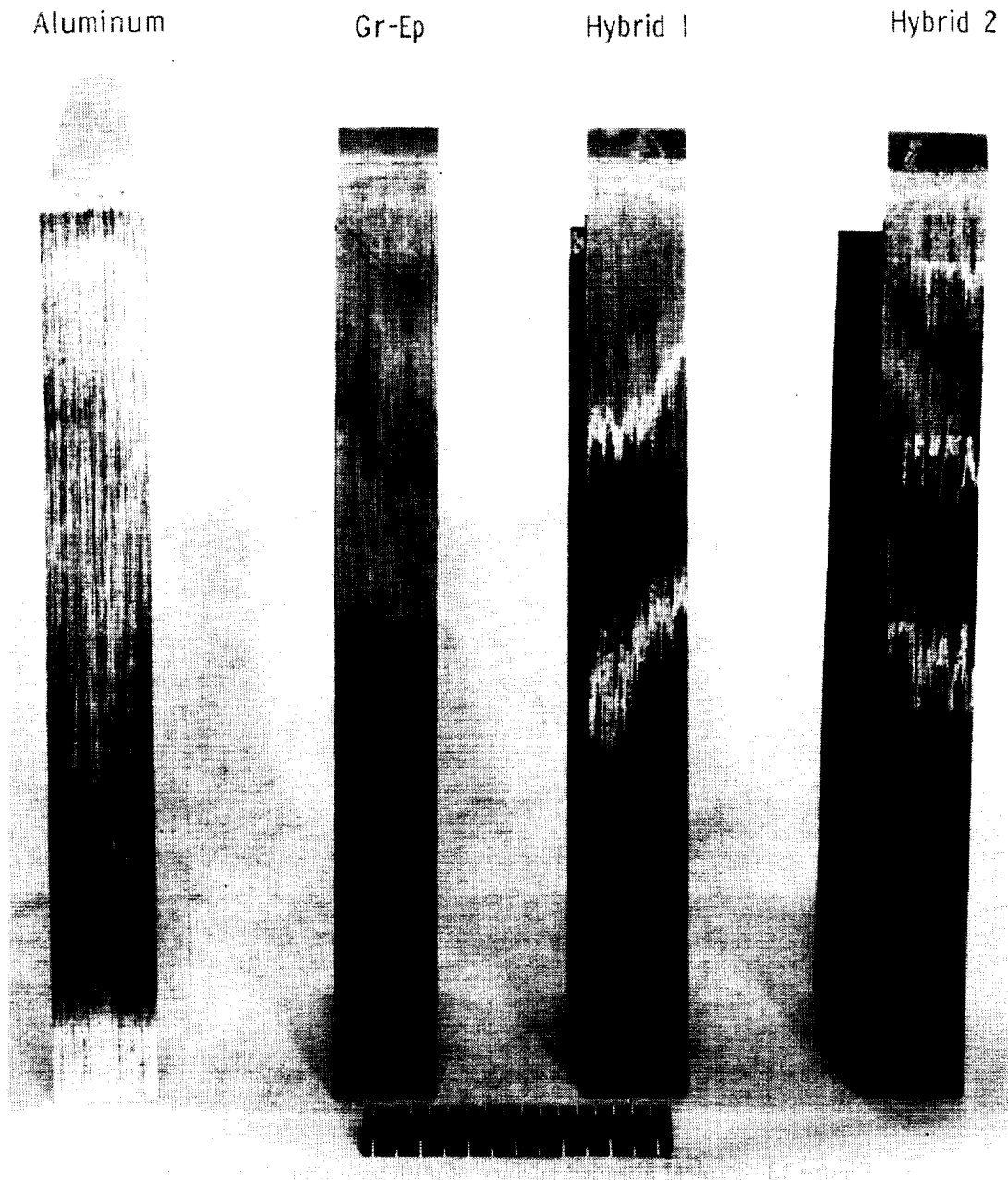


Aluminum



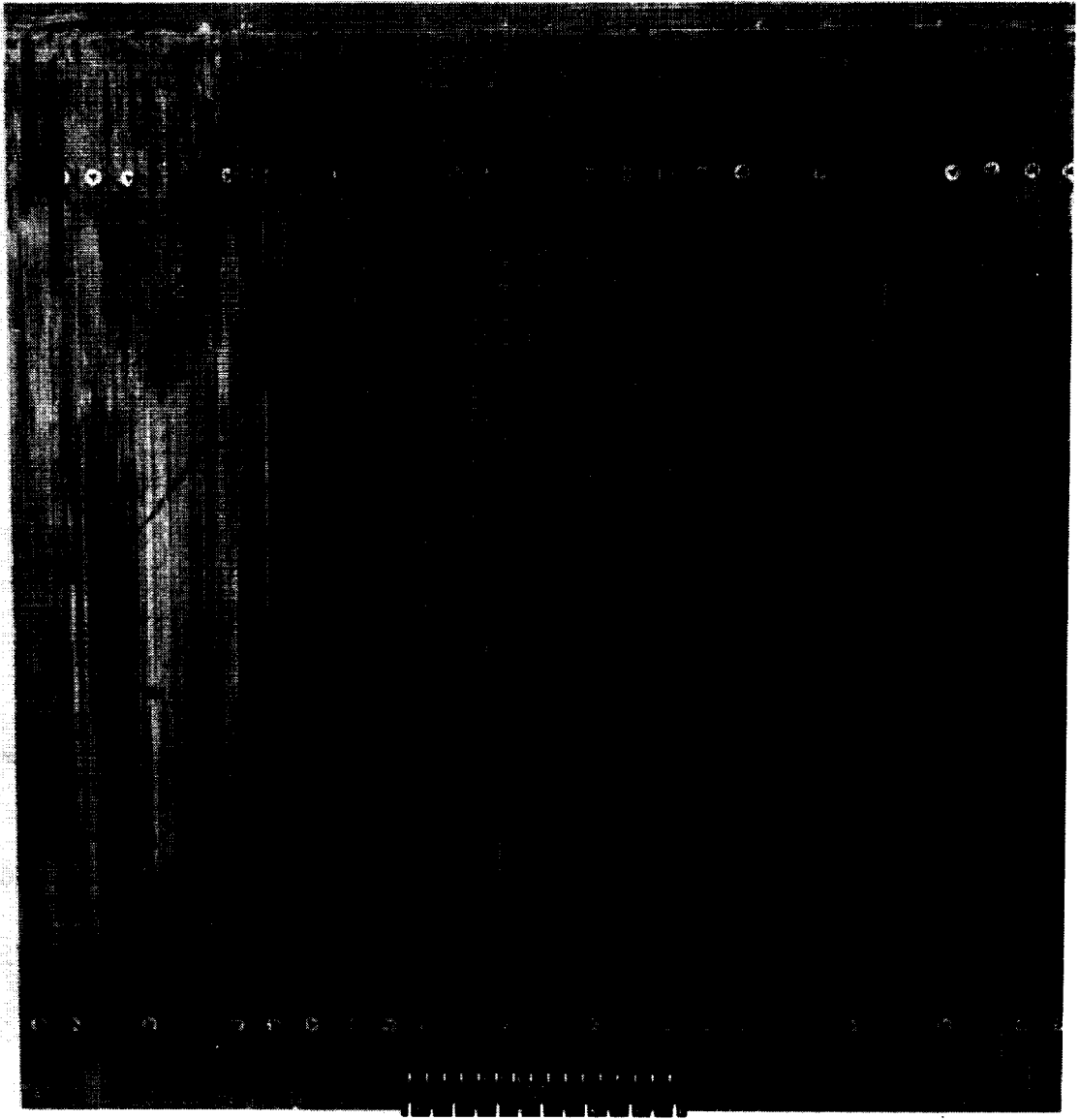
L-83-2408

Figure 11. General appearance of wear surface and wear debris particles for typical Kevlar, graphite-epoxy, and aluminum skin-coupon test specimens. Wear debris shown is not indicative of volume of wear for each specimen type.



L-84-13,735
Figure 12. Typical abraded surfaces of stiffened-skin test specimens.

↑
Front



L-85-3499

Figure 13. Typical abraded surface of stiffened-panel test specimen.

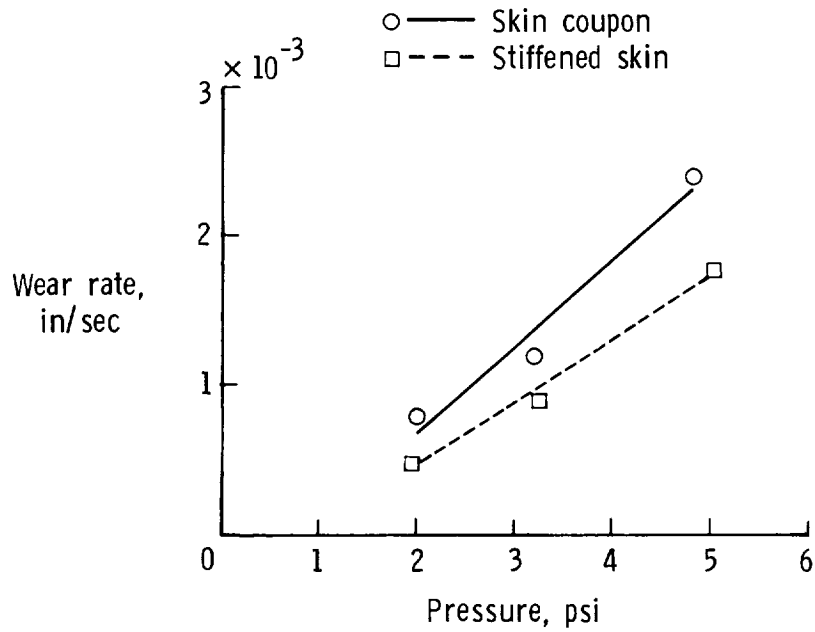


Figure 14. Wear rate of aluminum test specimens as a function of normal pressure for a test velocity of 32.5 mph.

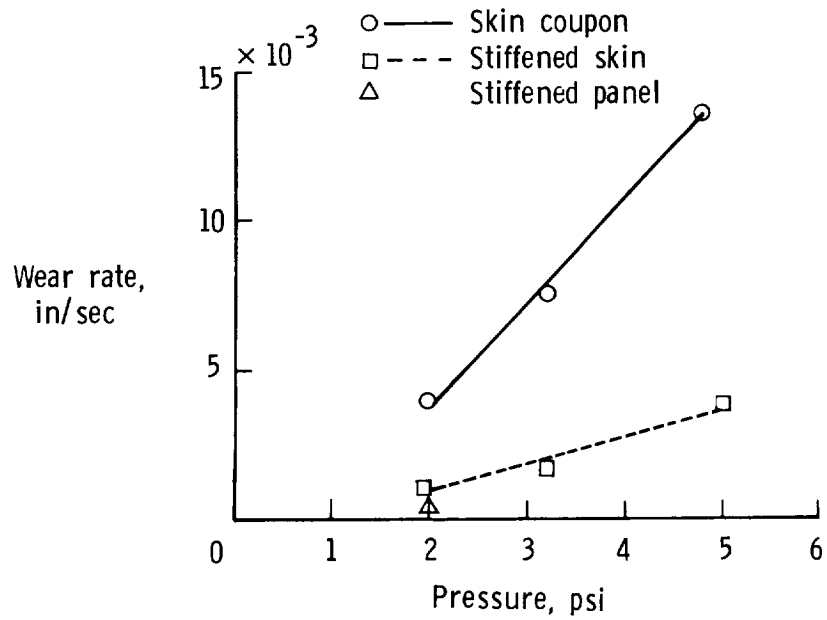


Figure 15. Wear rate of graphite-epoxy specimens as a function of normal pressure for a velocity of 32.5 mph.

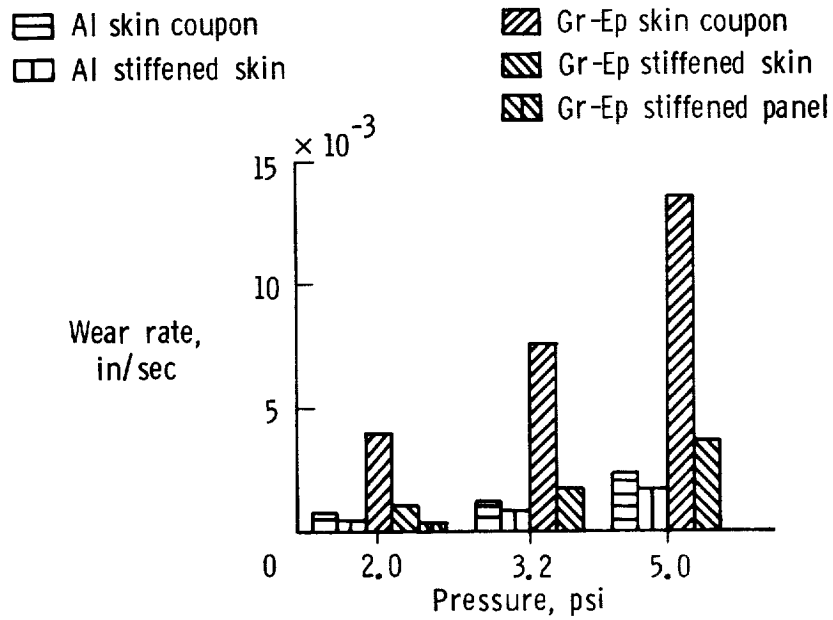


Figure 16. Comparisons of wear rate versus pressure for aluminum and graphite-epoxy (Gr-Ep) composite skin specimens for a test velocity of 32.5 mph.

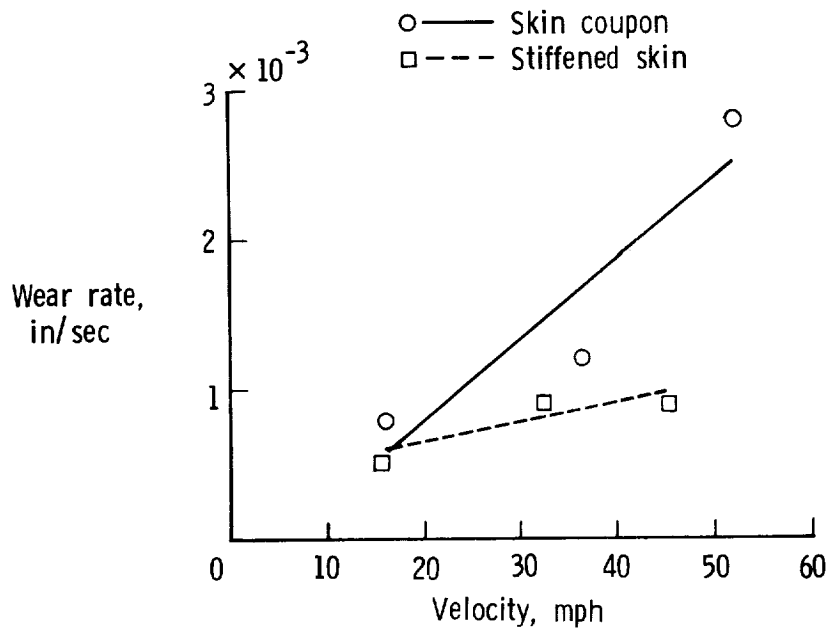


Figure 17. Wear rate of aluminum specimens as a function of velocity for a test pressure of 3.2 psi.

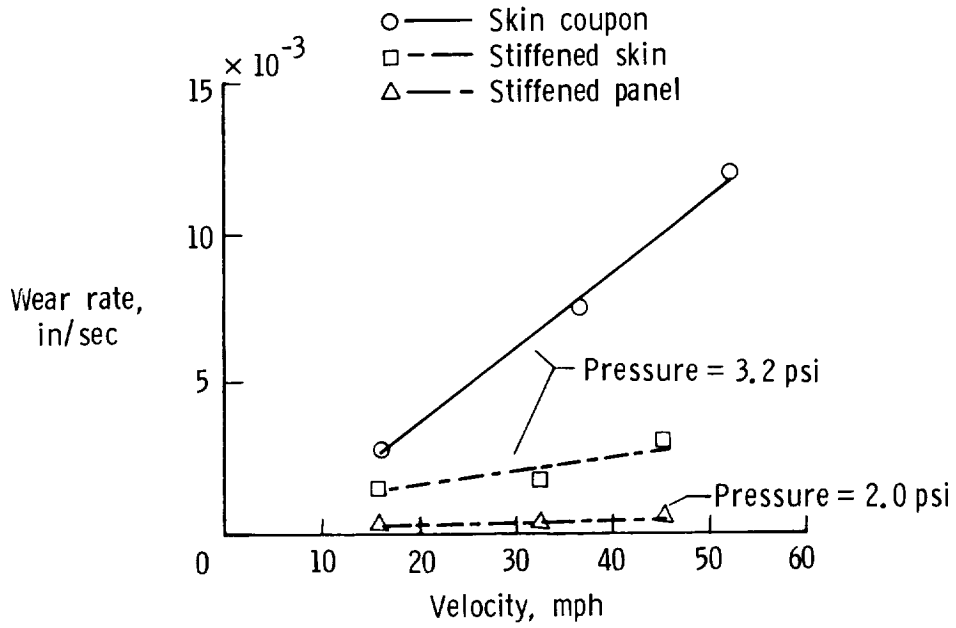


Figure 18. Wear rate of graphite-epoxy composite specimens as a function of velocity for a constant test pressure.

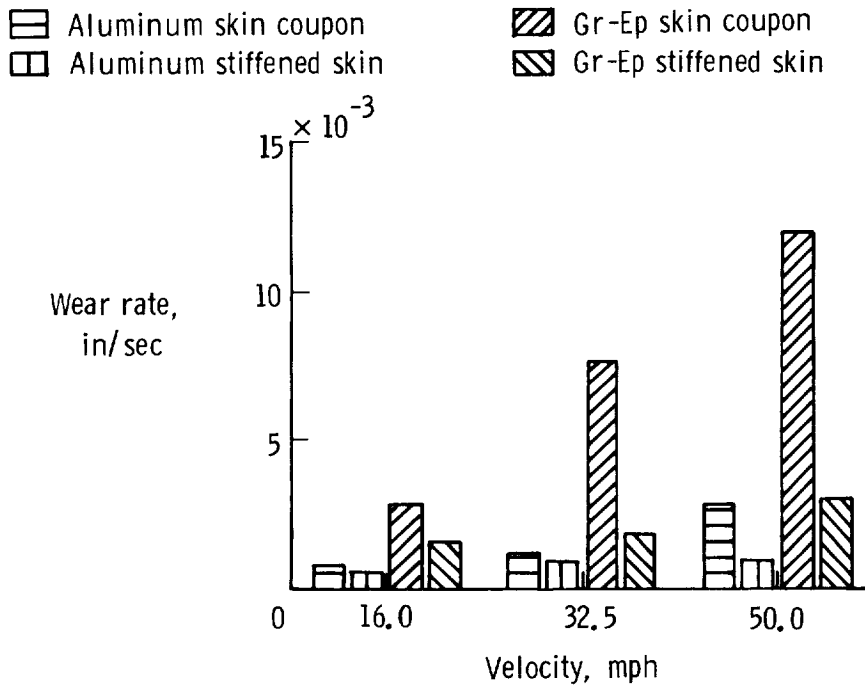


Figure 19. Comparisons of wear rate versus velocity for aluminum and graphite-epoxy (Gr-Ep) composite skin specimens for a test pressure of 3.2 psi.

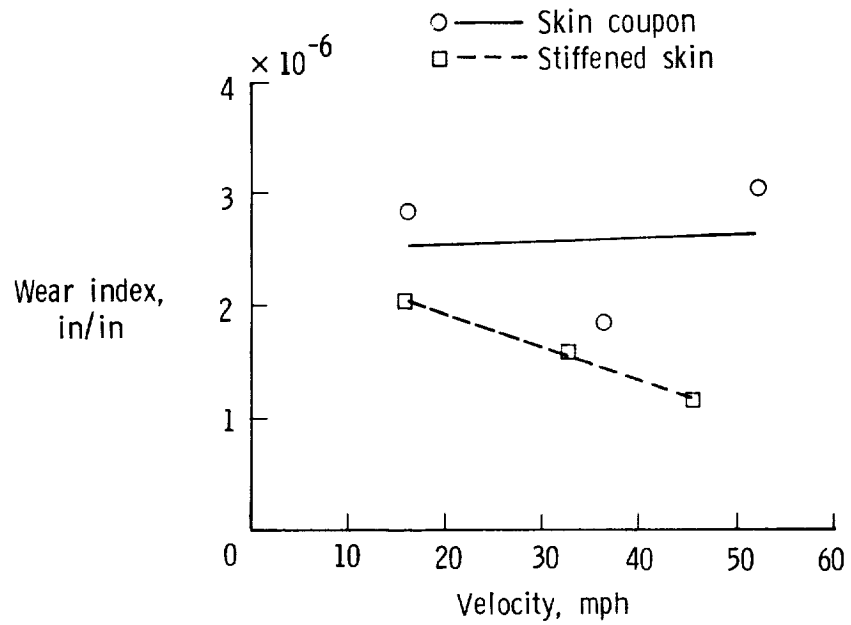


Figure 20. Wear index for aluminum specimens as a function of velocity for a test pressure of 3.2 psi.

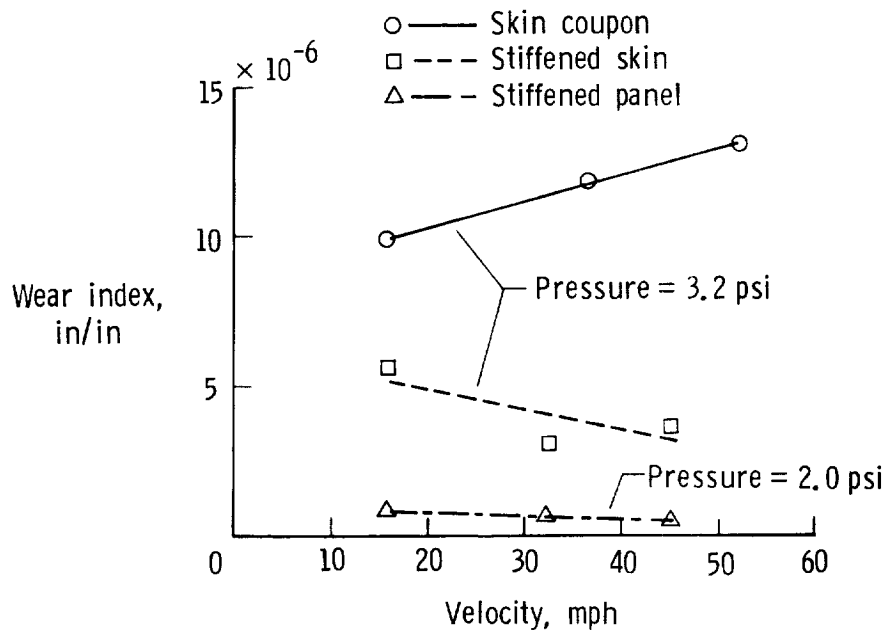


Figure 21. Wear index for graphite-epoxy specimens as a function of velocity for a constant test pressure.

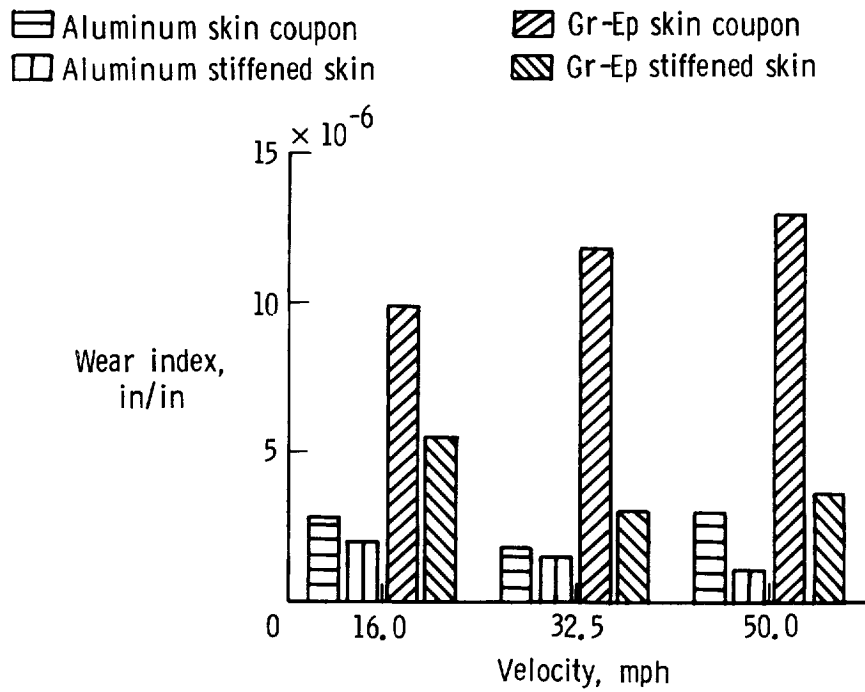


Figure 22. Wear index versus velocity for aluminum and graphite-epoxy (Gr-Ep) skin specimens for a test pressure of 3.2 psi.

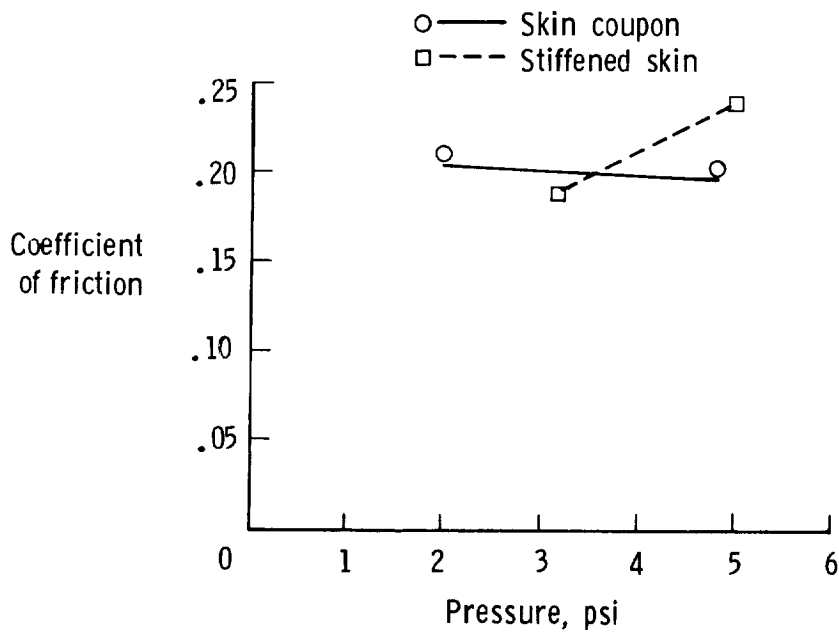


Figure 23. Coefficient of friction for aluminum specimens as a function of pressure for a constant test velocity of 32.5 mph.

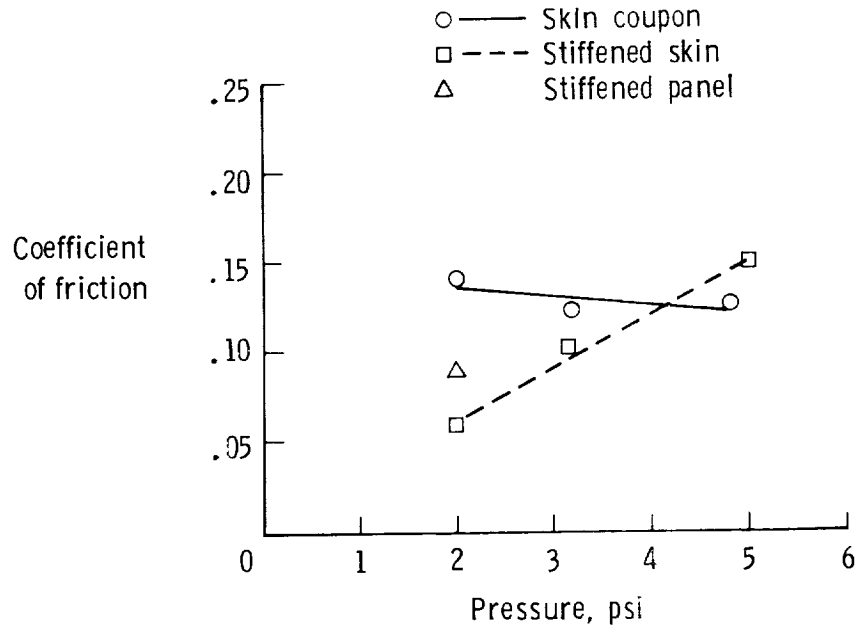


Figure 24. Coefficient of friction for graphite-epoxy specimens as a function of pressure for a constant test velocity of 32.5 mph.

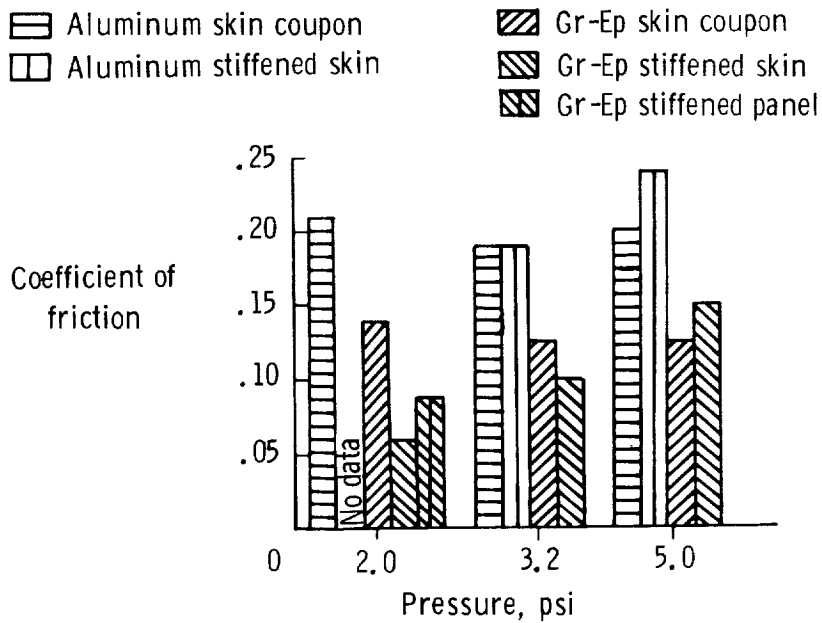


Figure 25. Coefficient of friction versus pressure for aluminum and graphite-epoxy (Gr-Ep) skin specimens at a constant test velocity of 32.5 mph.

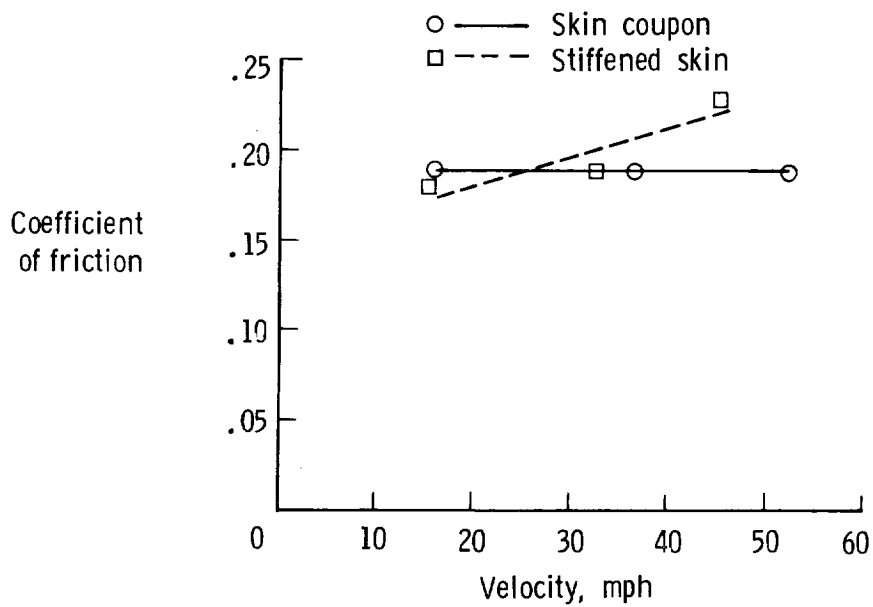


Figure 26. Coefficient of friction for aluminum specimens as a function of velocity for a constant test pressure of 3.2 psi.

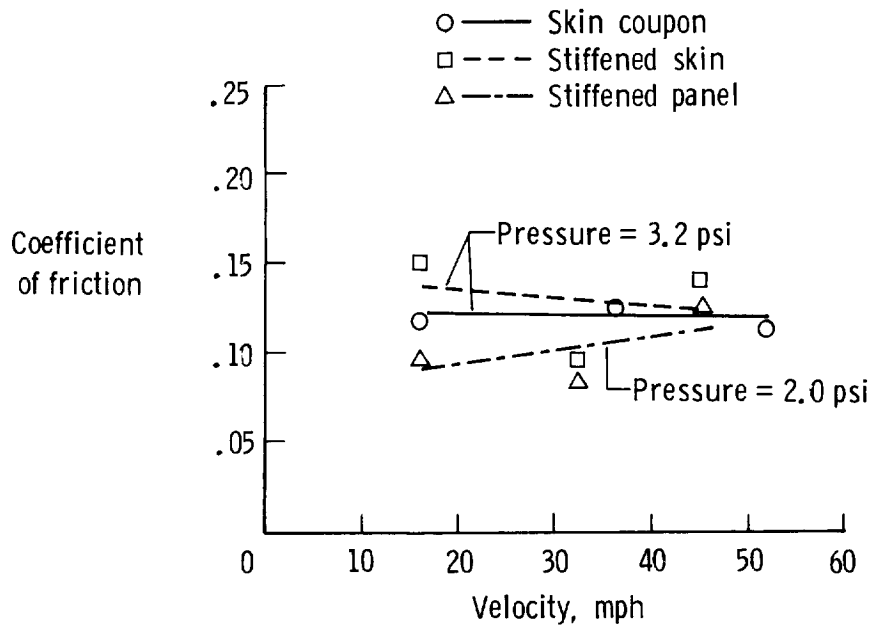


Figure 27. Coefficient of friction for graphite specimens as a function of velocity for a constant test pressure.

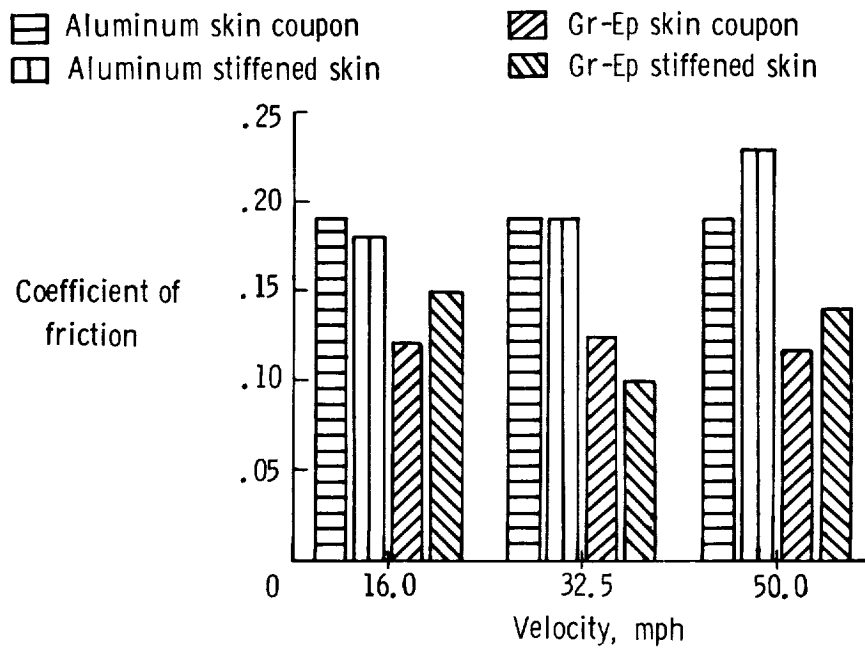


Figure 28. Coefficient of friction versus velocity for aluminum and graphite-epoxy (Gr-Ep) skin specimens for a test pressure of 3.2 psi.

1. Report No. NASA TP-2520 AVSCOM TR 85-B-7		2. Government Accession No.		3. Recipient's Catalog No.	
4. Title and Subtitle Abrasion Behavior of Aluminum and Composite Skin Coupons, Stiffened Skins, and Stiffened Panels Representative of Transport Airplane Structures				5. Report Date November 1985	
				6. Performing Organization Code 505-33-53-09	
7. Author(s) Karen E. Jackson				8. Performing Organization Report No. L-16018	
9. Performing Organization Name and Address Aerostructures Directorate USAARTA-AVSCOM Langley Research Center Hampton, VA 23665-5225				10. Work Unit No.	
				11. Contract or Grant No.	
				13. Type of Report and Period Covered Technical Paper	
12. Sponsoring Agency Name and Address National Aeronautics and Space Administration Washington, DC 20546-0001 and U.S. Army Aviation Systems Command St. Louis, MO 63120-1798				14. Army Project No. 1L161102AH45	
15. Supplementary Notes Karen E. Jackson: Aerostructures Directorate, USAARTA-AVSCOM.					
16. Abstract A three-phase investigation was conducted to compare the friction and wear response of aluminum and graphite-epoxy composite materials when subjected to loading conditions similar to those experienced by the skin panels on the underside of a transport airplane during an emergency belly landing on a runway surface. The first phase involved a laboratory test which used a standard belt sander to provide the sliding abrasive surface. Small skin-coupon test specimens were abraded over a range of pressures and velocities to determine the effects of these variables on the coefficient of friction and wear rate. The second phase involved abrading I-beam stiffened skins on an actual runway surface over the same range of pressures and velocities used in the first phase. In the third phase, large stiffened panels which most closely resembled transport fuselage skin construction were abraded on a runway surface. This report presents results from each phase of the investigation and shows comparisons between the friction and wear behavior of the aluminum and graphite-epoxy composite materials.					
17. Key Words (Suggested by Authors(s)) Abrasion of composites Friction and wear of metal and composites Composite airplane skin Toughened-resin composites			18. Distribution Statement Unclassified Unlimited Subject Category 05		
19. Security Classif.(of this report) Unclassified		20. Security Classif.(of this page) Unclassified		21. No. of Pages 31	22. Price A03